

Interference Analysis in Cooperative Multi-Hop Networks Subject to Multiple Flows

Quratulain Shafi* and Syed Ali Hassan†

School of Electrical Engineering and Computer Science
National University of Sciences and Technology, Islamabad, Pakistan
{10mscseqshafi*, ali.hassan†}@seecs.edu.pk

Abstract—This paper studies the effects of allowing multiple packets to flow simultaneously in a cooperative multi-hop transmission system. Although, the packet delivery rate may increase with multiple packet flows, however, the desired signals of one packet may get interfered with the signals of the other packets in the network, thereby causing some of the packets to die off. This phenomenon is analyzed by modeling the multi-hop transmission as a conditional Markov process, followed by the derivation of its transition matrix. The resulting distribution is used to calculate the outage probability of a node in a cooperative environment in the presence of desired as well as interfering signals. The model is then used to obtain the network coverage, until which a packet can travel for a given packet delivery ratio constraint. Numerical simulations are performed to validate the analytical models.

I. INTRODUCTION

IN a multi-hop Cooperative Transmission (CT), the resources of multiple, spatially separated radios are shared to transmit the data of a single source for improving link reliability and providing range extension by achieving transmit diversity [1]. The concept of Opportunistic Large Arrays (OLA) was introduced as a form of concurrent CT, that allows a group of nodes in each hop to transmit the same message to another group of nodes [1]. The benefits of this kind of network such as range extension [2] and energy efficiency [3] were deeply studied.

Infinite node density OLA transmissions (with single source packet) were initially studied using Monte-Carlo methods and successful infinite broadcast conditions were derived [1]. However, [4] studied the finite density extended networks and showed a zero probability of successful broadcast. An analytical model has been introduced for multi-hop cooperative linear networks with finite node density in [5], however, in this and other related works [6]–[8], only a single packet traverses the network and new packet is not allowed to be inserted into the network unless the previous packet reaches its destination. Interference due to multi packet OLA transmission within a single flow is studied, along a disk [9] as well as strip-shaped network [10]. However, in both these works, the authors assume that the sequence converges to a continuum limit, as the number of nodes in the network goes to infinity. This assumption is not appropriate for low density networks.

The authors gratefully acknowledge the National ICT RD Fund, Pakistan for sponsoring this research work.

When multiple packets are allowed to flow in a network simultaneously, transmission of one packet from one level to another, acting as a desired signal for one level may end up as an interfering signal for another, if these packets are transmitted over the same frequency reuse spectrum. We stochastically model the multi-flow, multi-hop network with a class of absorbing conditional Markov chains and prove numerically that the conditional Markov chain also exhibits a quasi-stationary distribution, and that Perron-Frobenius theorem holds for conditional Markov chain, if the random process is assumed to be homogeneous. We derive the outage probability of a node in the presence of desired as well as interfering signals. Expressions of outage probabilities based on Signal-to-Interference Ratio (SIR) exist in literature for a variety of channel models, including log-normal [11], Rayleigh and Rician [12] fading environments, all of which deal with single desired signal. The cumulative distribution function (CDF) of the ratio of sum of desired powers and the sum of interfering powers is required to obtain an expression of the outage probability, which to the best of the authors knowledge, is not present in literature.

Section II of this paper gives a detailed description of the network layout, while Sections III and IV present the proposed model of the network using conditional Markov chain and the derivation of its transition probability matrix, respectively. In Section V, the accuracy of the model is tested, followed by conclusion and possible future work in this particular subject.

II. SYSTEM DESCRIPTION

Consider a linear (one-dimensional) network topology with decode-and-forward (DF), half-duplex nodes placed d distance away from each other. Each level or hop consists of a fixed number, M , of nodes that cooperatively send the same message signal to the M nodes of next level as shown in Fig. 1, where $M = 4$. All the nodes that can decode the message, relay the message to the M nodes of the next level and this process continues until the message reaches the destination. We allow multiple packets to traverse the network simultaneously.

The source inserts a new data packet into the network and each packet takes one time slot to move from one level to the next. We assume perfect timing synchronization between the nodes of a level such that all the DF nodes of a level transmit

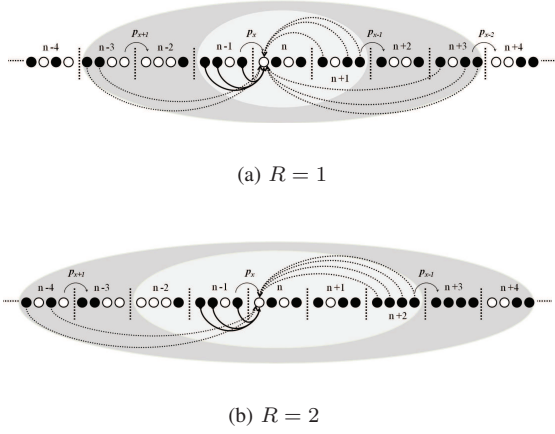


Fig. 1: Network topology for PIR 1 and 2, light gray area denotes tier 1 interference and dark gray area denotes additional interfering signals from tier 2.

at the same time over orthogonal fading channels [14]. Here, we define two network parameters; i) Packet Insertion Rate (PIR), R , and ii) tiers of interference, T . PIR is defined as the rate per time slot at which the source transmits a new packet. Since we assume half-duplex radios, a full rate transmission, $R = 1$, implies a packet insertion after waiting one time slot. For example, in Fig. 1(a), the DF nodes at level $(n - 1)$ transmit packet p_x to level n , where x represents the packet number being transmitted.¹ Similarly, level $(n + 1)$ transmits p_{x-1} to level $(n + 2)$, and so on. This is an example of *fastest possible* insertion rate. In Fig. 1(b), $R = 2$ implies that the source transmits a packet after waiting two time slots between consecutive transmissions. Therefore, when level $(n - 1)$ transmits p_x to level n , level $(n + 2)$ transmits p_{x-1} to level $(n + 3)$. Although, the intended destinations of level $(n - 1)$ nodes are level n nodes (for any R), however, assuming omnidirectional antennae, the transmissions will be overheard by the neighbouring levels, causing interference.

Solid arrows from level $(n - 1)$ to level n show the multiple desired signals, whereas, the dotted arrows represent the unwanted signals that occur because of multiple flows in the network. With different tiers, T , different number of levels interfere with the nodes of a level. As shown in Fig. 1(a), when $T = 1$, the unwanted signals affecting the node arrive only from level $(n + 1)$, whereas when $T = 2$, levels $(n + 3)$ and $(n - 3)$ also contribute to the interference with packet insertion rate, $R = 1$. When we increase R , the unwanted signals arrive from levels that are further away from the concerned node as shown in Fig. 1(b) where $R = 2$. Therefore, the interfering levels differ with different combinations of T and R .

A node at any certain level can decode and forward the packet without error when its received desired signal power and SIR are greater than thresholds, α and τ , respectively.

¹We have shown transmissions to one node only (namely, the first node of level n). However, all the nodes of level n receive the message from the DF nodes of level $(n - 1)$.

The filled black circles in Fig. 1 represent the DF nodes while the hollow circles show that the nodes have not decoded the data. The desired received power at the m th node of level n , denoted as $P_{r_m}(n)$ is given as $P_t \sum_{k=1}^K \frac{\mu_{km}}{(d_{km})^\beta}$, where we assume that all nodes of the network transmit with same transmit power, P_t . The channel gain, μ_{km} , from node k in the previous level to node m in the current level is exponentially distributed with unit mean and corresponds to the squared envelope of the signal undergoing Rayleigh fading. The distance d_{km} represents the Euclidian distance between the nodes and β is the path loss exponent. The summation is over the DF nodes of previous level such that $K \leq M$. SIR, φ , which is the ratio of desired and interfering power is given as

$$\varphi = \frac{\sum_{k=1}^K \frac{\mu_{km}}{(d_{km})^\beta}}{\sum_{i=1}^I \frac{\mu_{im}}{(d_{im})^\beta}}, \quad (1)$$

where K and I are the number of desired and interfering signals, respectively. We assume that the interfering signals also exhibit Rayleigh flat fading, where d_{km} and d_{im} are the distances between the node in the current level and the nodes in the previous and interfering levels, respectively.

III. MODELING BY CONDITIONAL MARKOV CHAIN

In this section, we propose the mathematical modeling of the network described in Section II with a class of discriminative model that forms a linear-chain conditional random field also known as conditional Markov chain [13]. Let $\mathcal{X}(n)$ denotes the state of the network at level n . A straight-forward way to model the state of the system is to represent the number of DF and non-DF nodes at level n . Let $\mathbf{1}_m(n)$ denotes the indicator function of a node m which takes value 1 when node m is a DF node and 0 when the node m could not decode the data. Hence the state of the system at level n can be represented as $\mathcal{X}(n) = [\mathbf{1}_1(n), \mathbf{1}_2(n), \dots, \mathbf{1}_m(n)]$, where $\mathcal{X}(n)$ is an M -bit binary word and each outcome is a state consisting of 2^M combinations in decimal form; $0, 1, \dots, 2^M - 1$. The state at level n can also be expressed as i_n . For example $i_n = 0101$ in binary and $i_n = 5$ in decimal form in Fig. 1(a).

As discussed previously, a node receives desired as well as interfering signals. Let \mathcal{Y} denotes the set of states that causes interference to the level under consideration. The states in \mathcal{Y} depend on the value of R and T . For example, \mathcal{Y} consists of levels $(n - 3)$, $(n + 1)$ and $(n + 3)$ when $R = 1$ and $T = 1$ as shown in Fig. 1(a). It can be shown that the cardinality of \mathcal{Y} , given as $|\mathcal{Y}| \leq \infty$ for a given tier, T and PIR, R . Based on these assumptions, the state of the system at level n i.e., $\mathcal{X}(n)$ depends on the previous state $\mathcal{X}(n - 1)$ and \mathcal{Y} . Hence $\mathcal{X}(n)$ conditional on $\mathcal{X}(n - 1)$ and \mathcal{Y} forms a conditional Markov chain [13], such that

$$\begin{aligned} \mathbb{P}\{\mathcal{X}(n) = i_n | \mathcal{X}(n - 1) = i_{n-1}, \dots, \mathcal{X}(1) = i_1, \mathcal{Y}\} \\ = \mathbb{P}\{\mathcal{X}(n) = i_n | \mathcal{X}(n - 1) = i_{n-1}, \mathcal{Y}\}. \end{aligned} \quad (2)$$

Here, the conditional Markov chain is homogeneous for a given T and R , with the assumption that the statistics of the

channel remains the same for all the hops in the network i.e., similar fading characteristics (Rayleigh fading) at each hop. This implies that if we fix R and T , similar system conditions can be observed at a later stage down the network. The PIR is generally fixed in the network. The motivation for fixing T is that we will later show that the increase in interfering tiers follows a diminishing returns phenomenon and considering additional interference tiers do not impact the network performance (e.g., outage probability of a node). This is because, after a sufficiently large T , the interfering levels are far apart from the level under consideration and are not contributing to the interference. It can be seen that all the nodes at a certain level can fail to decode the data successfully, thus forcing the Markov chain to go into an absorbing state (i.e., state 0 in decimal). This will result in the termination of the transmission for a particular packet, p_x . Therefore, the state space of the conditional Markov chain, \mathcal{X} , can be denoted as $\{0\} \cup S$, where $S = \{1, 2, \dots, 2^M - 1\}$, is the finite transient irreducible state space, while 0 is the absorbing state such that $\lim_{n \rightarrow \infty} \mathbb{P}\{\mathcal{X}(n) = 0\} \nearrow 1$ a.s. There always exists a probability for the transition of data from one transient state to another because of the irreducible state space S . We describe the conditional Markov chain in the form of two matrices. The first matrix, $\tilde{\mathbf{Q}}$, is the full, $2^M \times 2^M$ transition probability matrix for the states in the set $\{0\} \cup S$, in which each row sums to one. We cross out the columns and rows that involve the transitions to and from state 0 in $\tilde{\mathbf{Q}}$ to form the second matrix, \mathbf{Q} , making a $(2^M - 1) \times (2^M - 1)$ submatrix of $\tilde{\mathbf{Q}}$, that corresponds to the states in S . It can be construed here that the transition probability matrix, \mathbf{Q} , is not true stochastic, as its row entries do not sum to 1. Moreover, \mathbf{Q} being a square irreducible non-negative matrix inevitably results in the existence of an eigenvalue, ρ , according to Perron-Frobenius theorem such that, $\{0 < \rho < 1\}$. The theory of Markov chains states that a distribution $\mathbf{u} = (u_i, i \in S)$ is called ρ -invariant distribution if \mathbf{u} is the left eigenvector of the transition matrix, \mathbf{Q} , corresponding to ρ , i.e., $\mathbf{u}\mathbf{Q} = \rho\mathbf{u}$.

As time proceeds, the limiting behaviour of the Markov chain portrays that termination of the transmission of data or in other words killing is an inevitable event, since $\forall n, \mathbb{P}\{\mathcal{X}(n) = 0\} > 0$. However, we are interested in finding the distribution of the transient states, just before the absorbing state is reached. This limiting distribution is known as the quasi-stationary distribution of the Markov chain, and is independent of the initial conditions of the process. From [5] the ρ -invariant distribution for one-step transition probability matrix of the Markov chain on S provides this unique distribution. To find the quasi-stationary distribution, we first calculate the maximum eigenvector, $\hat{\mathbf{u}}$, of \mathbf{Q} . Defining $\mathbf{u} = \hat{\mathbf{u}} / \sum_{i=1}^{2^M-1} \hat{u}_i$, as a normalized version of $\hat{\mathbf{u}}$ that sums to one gives the quasi-stationary distribution of \mathcal{X} . Hence the unconditional probability of being in state r at level n is given as

$$\mathbb{P}\{\mathcal{X}(n) = r\} = \rho^n u_r, \quad r \in S, \quad n \geq 0. \quad (3)$$

We also let $E = \inf\{n \geq 0 : \mathcal{X}(n) = 0\}$ denote the

level at which the killing occurs. It follows then, $\mathbb{P}\{E > n + n_0 | E > n\} = \rho^{n_0}$, while the quasi-stationary distribution of the Markov chain is $\lim_{n \rightarrow \infty} \mathbb{P}\{\mathcal{X}(n) = r | E > n\} = u_r$, where $r \in S$. This equation represents the conditional probability of being in a state r given that the killing state has not arrived yet. This conditional probability is just the r th value of the eigenvector of matrix \mathbf{Q} .

IV. TRANSITION PROBABILITY MATRIX

In this section, we find the state transition probability matrix, \mathbf{Q} , for our model, the eigenvector of which will give us the quasi-stationary distribution. The probability for a node m to decode at level n is

$$\begin{aligned} & \mathbb{P}\{\text{node } m \text{ of level } n \text{ will decode}\} \quad (4) \\ &= \mathbb{P}\{\mathbb{I}_m(n) = 1\} = \mathbb{P}\{P_{r_m}(n) \geq \alpha \cap \varphi_m(n) \geq \tau\}, \end{aligned}$$

where $P_{r_m}(n)$ and $\varphi_m(n)$ represent the received power and the received SIR respectively, for the m th node at level n . The success probability of the node is given as

$$\begin{aligned} & \mathbb{P}\{P_{r_m}(n) \geq \alpha \cap \varphi_m(n) \geq \tau\} \quad (5) \\ &= \int_{x=\alpha}^{\infty} \left[\int_{y=0}^{x/\tau} f_{\varphi_m}(y) dy \right] f_{P_{r_m}}(x) dx, \end{aligned}$$

where $f_{P_{r_m}}(x)$ and $f_{\varphi_m}(y)$ are the probability distribution functions (PDFs) of the received power and the received SIR at the m th node, respectively. The nodes exhibit a performance threshold, where data received at a certain node is decoded successfully only when both the received power, P_r , and SIR, φ , exceed certain defined thresholds, denoted by α and τ , respectively. Assuming a Rayleigh fading environment, both the desired and the interfering powers are exponentially distributed. Hence the numerator of (1) represents a random variable which is a sum of K independent but non-identically distributed (i.n.i.d) exponential RVs. Same phenomenon goes for the denominator of (1). The resulting distribution for the sum of K desired powers and for the sum of I interfering powers are both hypoexponential distributions as given in the following definition.

Definition 1. A RV $X \sim$ hypoexponential ($\boldsymbol{\lambda}$) with positive parameter vector $\boldsymbol{\lambda} = \lambda_1, \lambda_2, \dots, \lambda_k$, such that $\lambda_k \neq \lambda_j$, if X is a sum of mutually independent exponential RVs, X_1, X_2, \dots, X_k with respective parameters $\lambda_1, \lambda_2, \dots, \lambda_k$.

To obtain an expression of the outage probability, the Cumulative Distribution Function (CDF), $F_Z(z)$, of the ratio of sum of desired powers and the sum of interfering powers is required, which is derived in the following theorem.

Theorem 1 (Ratio of independent hypoexponential random variables). Let $X \sim$ hypoexponential ($\boldsymbol{\lambda}$) and $Y \sim$ hypoexponential ($\boldsymbol{\eta}$) be two independent hypoexponential RVs and let $Z = X/Y$. The Complementary Cumulative Distribution Function (CCDF) of Z is given as

$$\mathbb{P}\{Z > \tau\} = \sum_{i=1}^I \sum_{k=1}^K C_i D_k \left(\frac{\lambda_k}{\tau \eta_i + \lambda_k} \right), \quad (6)$$

where

$$C_i = \prod_{j=1, j \neq i}^I \frac{\eta_i}{\eta_i - \eta_j}, \quad D_k = \prod_{l=1, l \neq k}^K \frac{\lambda_k}{\lambda_k - \lambda_l}. \quad (7)$$

Proof. Each X and Y is a sum of independent exponential RVs, such that $X = X_1 + X_2 + X_3 + \dots + X_K$ and $Y = Y_1 + Y_2 + Y_3 + \dots + Y_I$. As X_k and Y_i both have exponential distribution, hence $f_\zeta(u) = \frac{1}{\phi} \exp\left(\frac{-u}{\phi}\right)$, where $\zeta \in \{X_k, Y_i\}$ with respective parameters $\phi \in \{\lambda_k, \eta_i\}$ such that $\lambda_k \neq \eta_i, \forall i, k$. The hypoexponential distribution of X is given as

$$f_X(x) = \sum_{k=1}^K D_k \frac{1}{\lambda_k} \exp\left(\frac{-x}{\lambda_k}\right), \quad (8)$$

Similarly, the distribution of Y is also hypoexponential as given in (7) with λ_k replaced with η_i and D_k with C_i . Since X and Y are independent, the CDF of the ratio of $Z = X/Y$ is obtained by integrating the original PDFs on the region of support, i.e., $\mathbb{P}\{Z \leq \tau\} = 1 - \mathbb{P}\{Z > \tau\} = 1 - \mathbb{P}\{X/Y > \tau\}$. Therefore,

$$\mathbb{P}\{X/Y > \tau\} = \int_{x=0}^{\infty} \left[\int_{y=0}^{x/\tau} f_Y(y) dy \right] f_X(x) dx, \quad (9)$$

The term under square brackets is the CDF of hypoexponential RV and is given as

$$\int_{y=0}^{x/\tau} f_Y(y) dy = \sum_{i=1}^I C_i \left[1 - \exp\left(-\frac{x}{\tau \eta_i}\right) \right]. \quad (10)$$

By combining (7) and (11), (9) is evaluated as

$$\mathbb{P}\{Z > \tau\} = \sum_{i=1}^I \sum_{k=1}^K C_i D_k \left(\frac{\lambda_k}{\tau \eta_i + \lambda_k} \right). \quad (11)$$

Now we are in a position to derive the success probability of a node given by (4), where we assume that the received power, P_r is required to be greater than α , which requires changing the lower limit of x in (9) to α . Thus the probability of success is given as

$$\mathbb{P}\{Z > \tau\} = \sum_{i=1}^I \sum_{k=1}^K \frac{C_i D_k}{\lambda_k} \int_{x=\alpha}^{\infty} \left[\exp\left(\frac{-x}{\lambda_k}\right) - \exp\left(\frac{-x}{\lambda_k} - \frac{-x}{\tau \eta_i}\right) \right] dx, \quad (12)$$

which after a straight-forward analysis gives

$$\mathbb{P}\{Z > \tau\} = \sum_{i=1}^I \sum_{k=1}^K C_i D_k \exp\left(\frac{-\alpha}{\lambda_k}\right) \left[1 - \frac{\tau \eta_i}{\tau \eta_i + \lambda_k} \exp\left(\frac{-\alpha}{\tau \eta_i}\right) \right]. \quad (13)$$

Until now, the number of interfering nodes are represented by I , where $I \in \mathbb{Z}^+$, \mathbb{Z}^+ being the set of positive integers. However, in the network of Fig. 1, the number of interfering

nodes depends upon R and T . Hence, we represent an interfering level as $(n + \gamma_j)$ where $\gamma_j \in \Gamma$ and $j \in \{1, 2, \dots, |\Gamma|\}$, where $|\Gamma|$ is the cardinality of set Γ . The set Γ depends on the values of R and T , such that $\Gamma = \{1\}$ when $R = 1$ and $T = 1$, whereas $\Gamma = \{1, 3, -3\}$ when $R = 1$ and $T = 2$ as shown in Fig. 1. We define two sets, \mathbb{K} and \mathbb{I} , to represent the indices of the nodes that are active in the desired and interfering levels, respectively, where $|\mathbb{K}| \leq M$. However, as $|\Gamma| \geq 1$, there might be different indices for each interfering level, making $|\mathbb{I}| \leq M|\Gamma|$. We can now express, the probability of success of the m th node at level n as

$$P_s^{(m)} = \sum_{\substack{i \in \mathbb{I}_{(n+\gamma_j)}, \\ \gamma_j \in \Gamma}} \sum_{k \in \mathbb{K}_{(n-1)}} C_i D_k \exp\left(\frac{-\alpha}{\lambda_k^{(m)}}\right) \left[1 - \frac{\tau \eta_{i, \gamma_j}^{(m)}}{\tau \eta_{i, \gamma_j}^{(m)} + \lambda_k^{(m)}} \exp\left(\frac{-\alpha}{\tau \eta_{i, \gamma_j}^{(m)}}\right) \right], \quad (14)$$

where C_i and D_k are given in (8), $\lambda_k^{(m)}$ is the coefficient of the exponential RV from node k in the desired level $(n-1)$ to node m in the current level n , and $\eta_{i, \gamma_j}^{(m)}$ is the coefficient of the exponential RV from node i in the interfering level $(n+\gamma_j)$ to the m th node in the current level n given as

$$\lambda_k^{(m)} = \frac{1}{d^\beta (M - k + m)^\beta}, \quad (15)$$

and

$$\eta_{i, \gamma_j}^{(m)} = \begin{cases} \gamma > 0, & \frac{1}{d^\beta (M|\gamma_j| - m + i)^\beta} \\ \gamma < 0, & \frac{1}{d^\beta (M|\gamma_j| - i + m)^\beta}. \end{cases} \quad (16)$$

We represent the states of the desired level, $(n-1)$ and current level, n as s_1 and s_2 such that $\{s_1, s_2\} \in S$. The state of interfering levels, on the other hand belongs to $\{0\} \cup S$, as there is a possibility that all the nodes in an interfering level fail to decode data from their respective desired levels, causing no interference for the level under consideration. For a given R and T , we have $|\Gamma|$ interfering levels, hence the total possible number of combinations of interfering level states become $(2^M)^{|\Gamma|}$. If we assume that all the interfering levels are equally likely, the transition probability will be an average of all the probabilities over all the combinations of interfering level states. If we let the indices of those nodes that decode the data correctly in state s_2 (at level n) and indices of those that fail to decode, to be $\mathbb{N}_n^{(s_2)}$ and $\bar{\mathbb{N}}_n^{(s_2)}$, respectively, the probability, P_ϑ for interfering combination ϑ is given as

$$P_\vartheta = \prod_{m \in \mathbb{N}_n^{(s_2)}} \left(P_s^{(m)} \right) \prod_{m \in \bar{\mathbb{N}}_n^{(s_2)}} \left(1 - P_s^{(m)} \right), \quad (17)$$

where $P_s^{(m)}$ is given in (14) and the combination ϑ dictates the set \mathbb{I} . Finally, we deduce one-step transition probability for going from state s_1 to state s_2 given interfering set \mathbb{A} , where \mathbb{A} represents all possible combinations of interfering levels as

$$P_{s_2|s_1, \mathbb{A}} = \sum_{\vartheta \in \mathbb{A}} \frac{P_\vartheta}{(2^M)^{|\Gamma|}}. \quad (18)$$

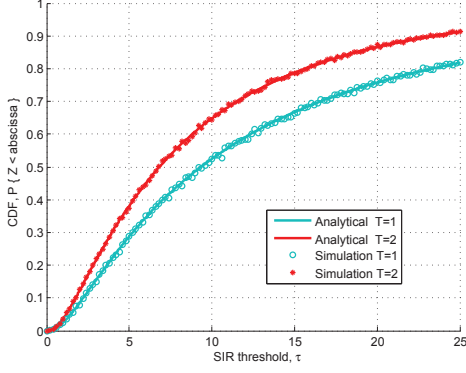


Fig. 2: CDF of the ratio of two hypoexponential RVs for $M = 2$, $R = 1$.

The state transition probabilities are used to formulate a $(2^M - 1) \times (2^M - 1)$ matrix, \mathbf{Q} , that we mentioned in Section III. The eigenvector of \mathbf{Q} will give us the quasi-stationary distribution.

V. RESULTS

In this section, we present various results pertaining to the performance of the cooperative network under multiple flows. First of all we present the analytical as well as numerical simulation results to show the validity of Theorem 1, i.e., the ratio of independent hypoexponential RVs. We assume the network topology as shown in Fig. 1, to compare the results of the CDF, $\mathbb{P}\{Z < \tau\}$, for $M = 2$ and $R = 1$. It can be seen in Fig. 2 that the analytical and numerical results match closely for both the tiers. The analytical results are obtained from (7) and the solid curve shows the outage probability (i.e., the CDF) of a single node (specifically the first node of level n) in the presence of desired as well as interfering signals. For a fixed τ , the outage probability increases when we move from tier 1 to tier 2, as tier 2 introduces more interfering signals to the node under consideration. In all the results, we set $d = 1$ and $\beta = 2$.

Fig. 3 shows the comparison of distribution of states for analytical and simulation model for $M = 2$, $R = 1$ and $T = 1$, with $\alpha = 0.1$ and $\tau = 0.05$ for various number of hops. When $M = 2$, there are potentially three transient states in the system, which are $\{0, 1\}$, $\{1, 0\}$ and $\{1, 1\}$. The figure represents the probability of being in each state using the analytical as well as the simulation model. The analytical part is attained using (18), whereas for the simulation results, we randomly generate the states initially and then assign 1 or 0 to each node of the next level, if the received power and SIR are greater or less than the thresholds α and τ , respectively. This process continues until all the nodes fail to decode in a level (i.e., the absorbing state is reached). We then take the average of 100,000 simulation trials. It can be noted that with the increase in the number of hops, the probability of each transient state also decreases, however the skewness of all the three curves remains constant. This plot shows that

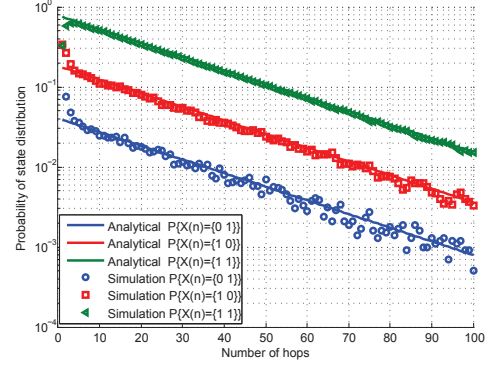


Fig. 3: Distribution of the states for $M = 2$, $R = 1$, $T = 1$, $\alpha = 0.1$, $\tau = 0.05$.

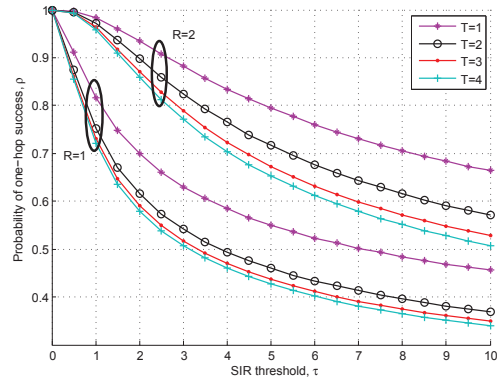


Fig. 4: Probability of one-hop success for $M = 2$, $\alpha = 0.05$.

the quasi-stationary property is exhibited by the conditional Markov chains. It can be noted that initially the possibility of state distribution is equally likely for the simulation results, i.e., $1/3$. However, after a few hops, the network achieves the quasi-stationary distribution for a given R and T .

The probability of one-hop success, ρ , is the Perron-Frobenius eigenvalue of the matrix \mathbf{Q} that represents the probability of at least one node decoding the data. Fig. 4 represents ρ versus SIR threshold, τ for various tiers of interfering signals, where $\alpha = 0.05$ and $M = 2$. For a certain τ , the probability of one-hop success decreases when we move from $T = 1$ to $T = 2$, and similarly for $T = 2$ to $T = 3$ and so on, as more interfering signals are introduced. However, the effect of increasing interference tiers show diminishing returns. Therefore, for this network topology, the effect of interference on the performance of a node is noticeable for upto two-tier levels of interference only. Same effect can be seen for $R = 2$, with the exception that this case shows better success probability for a fixed τ . This is because when PIR is higher, the interfering tiers are spread further apart resulting in a reduced outage probability. The quality of service (QoS), η of this type of network can be represented as the probability of

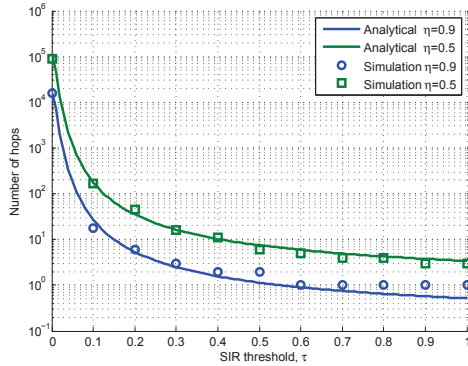


Fig. 5: Number of hops for $M = 2$, $R = 1$, $T = 1$, $\alpha = 0.01$.

not having entered the absorbing state, making its ideal value 1. Equation (3) provides the maximum number of hops, h , that a packet can travel for a given η , i.e., $\rho^h \geq \eta$, which gives $h \leq \frac{\ln \eta}{\ln \rho}$. If the required QoS is decreased, the coverage of the network increases as shown in Fig. 5, in which we show the analytical and simulation results for τ versus the number of hops, h that can be reached, which specifies the number of level until which the packet travels with a packet delivery rate (PDR) of η . In Fig. 5, $M = 2$, $R = 1$, $T = 1$ and $\alpha = 0.01$. For the simulation results, we run the simulation for 100,000 packets and observe the hop number at which the packet delivery ratio equals the value of η .

Fig. 6 shows the distance that can be covered over a range of required SIR threshold, τ , for various values of PIRs and M , where $\alpha = 0.01$. The distance is represented as normalized distance, which is evaluated by multiplying the number of hops, h , and the number of nodes in a certain level, M , and then dividing by d . Higher value of R shows that the network waits for more time slots before inserting another packet, reducing the interference at a certain level for a given tier ($T = 1$ in this case), providing larger network coverage. Lowering R improves the networks throughput due to higher simultaneous packet transmission; but packets may be lost owing to interference. Thus, to attain a certain QoS, a trade off between the two is required. As we increase the number of nodes in each hop, better coverage can be attained for a certain value of τ , indicating the effects of increased diversity gain. It can be further observed that same distance might be achieved for various combinations of M and R . For instance, at $\tau = 0.4$, same coverage of the network can be achieved if $M = 4$, $R = 2$ or $M = 3$, $R = 3$. The former case has a higher throughput and less delay (owing to larger hop distance) and may be preferred over the latter case.

VI. CONCLUSION

Interference due to multiple flows in a cooperative linear network is modeled using conditional Markov chain, where the desired and interfering signals are non-identical and exponentially distributed. Expression for the outage probability of

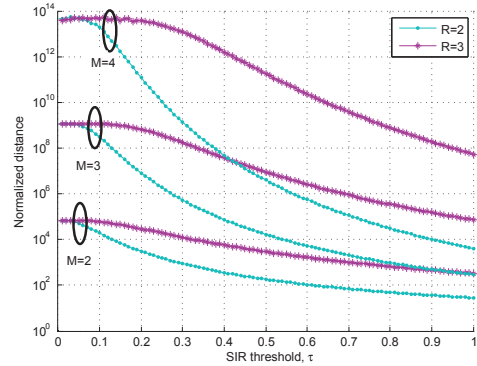


Fig. 6: Coverage of network for $T = 1$, $\alpha = 0.01$, $\eta = 0.9$.

a node is derived based on received power and received signal-to-interference ratio by determining the CDF of the ratio of two hypoexponential RVs. Analytical and simulation results are presented to show the accuracy of the proposed model, as well as to observe the effect of increasing interference on the outage probability, by varying packet insertion rate and tiers of the interference.

REFERENCES

- [1] B. S. Mergen, A. Scaglione, and G. Mergen, "Asymptotic analysis of multi-stage cooperative broadcast in wireless networks," *IEEE Trans. Inform. Theory*, vol. 52, no. 6, pp. 2531-2550, 2006.
- [2] M. Bacha and S. A. Hassan, "Distributed versus Cluster-Based Cooperative Linear Networks: A Range Extension Study in Suzuki Fading Environments," *In Proc. IEEE Personal Indoor and Mobile Radio Communications (PIMRC)*, 2013, London, UK.
- [3] R. I. Ansari and S. A. Hassan, "Opportunistic Large Array with Limited Participation: An Energy-Efficient Cooperative Multi-Hop Network," *IEEE International Conference on Computing, Networking and Communications (ICNC)*, 2014, Hawaii, United States.
- [4] C. Capar, D. Goeckel and D. Towsley, "Broadcast analysis for large cooperative wireless networks," arXiv preprint arXiv:1104.3209 (2011).
- [5] S. A. Hassan and M. A. Ingram, "A quasi-stationary Markov chain model of a cooperative multi-hop linear network," *IEEE Trans. Wireless Commun.*, vol. 10, no. 7, pp. 2306-2315, 2011.
- [6] A. Afzal and S. A. Hassan, "Stochastic Modeling of Cooperative Multi-Hop Strip Networks with Fixed Hop Boundaries," *IEEE Transactions on Wireless Communications*, vol. 13, no.8, pp. 4146-4155, Aug. 2014.
- [7] M. Bacha and S. A. Hassan, "Performance Analysis of Cooperative Linear Networks Subject to Composite Shadowing Fading," *IEEE Transactions on Wireless Communications*, vol. 12, no. 11, pp. 5850-5858, Nov. 2013.
- [8] S. A. Hassan, "Performance Analysis of Cooperative Multi-hop Strip Networks," *Springer Wireless Personal Communications*, vol. 74, no. 2, pp. 391-400, 2014.
- [9] H. Jung and M. A. Ingram, "Analysis of spatial pipelining in Opportunistic Large Array broadcasts," *in Proc IEEE MILCOM*, pp. 991-996, 2011.
- [10] H. Jung and M. A. Ingram, "Analysis of intra-flow interference in opportunistic large array transmission for strip networks," *in Proc. IEEE ICC*, pp. 104-108, 2012.
- [11] G. L. Stüber, *Principles of Mobile Communication*, Springer New York, 2011.
- [12] Y. D. Yao and A. U. H. Sheikh, "Outage probability analysis for micro-cell mobile radio systems with cochannel interferers in Rician/Rayleigh fading environment," *Electron. Lett.*, vol. 26 no. 13, pp. 864-866, 1990.
- [13] M. Sinn and B. Chen, "Central limit theorems for conditional markov processes," *J. Machine Learning Research*, vol. 31, pp. 554-562, 2013.
- [14] S. S. Syed and S. A. Hassan, "On the use of space-time block codes for Opportunistic Large Array network," *in Proc. IEEE Int. Wireless Commun. and Mobile Computing Conf. (IWCMC)*, Aug., 2014, Nicosia, Cyprus.